

highest elevations. (The value of seven was calculated from the total effect of a factor of 20 by the removal of an approximately threefold difference in the weathering rate due to differences in mean annual temperature at the two elevations.)

For reasonable ranges of values, other factors affected atmospheric CO<sub>2</sub> concentrations during the Paleozoic much less than those that resulted from changes in solar radiation or from plant evolution. These factors include changes in CO<sub>2</sub> degassing that accompanied changes in seafloor spreading, changes in the mean relief of the continents as indicated by the oceanic <sup>87</sup>Sr/<sup>86</sup>Sr ratio, changes in land area subject to weathering, and changes in global river runoff. Most of these factors are tectonic in origin, which suggests that tectonics was overshadowed by solar and plant evolution as a major control of atmospheric CO<sub>2</sub> concentration during the Paleozoic but not at later times.

The CO<sub>2</sub> values calculated for the Paleozoic era agree with independently derived results from the carbon isotopic study of paleosols (Fig. 3) (2, 3). There is little doubt that the atmospheric CO<sub>2</sub> concentration during the early Paleozoic was considerably higher than it is today and that it probably dropped as vascular plants arose and accelerated the rate of CO<sub>2</sub> uptake by weathering. These plants had a double effect. In addition to accelerating weathering, they provided a new source of bacterially resistant organic matter (for example, lignin) for burial in sediments. As a result, the removal of atmospheric CO<sub>2</sub> by the massive burial of sedimentary organic matter during the Carboniferous and Permian periods (21, 22), evidenced by the abundance of coal of this age, amplified the large mid-Paleozoic drop in CO<sub>2</sub> concentration. The consequently lowered greenhouse effect from this drop likely had a major influence in bringing about the Permian-Carboniferous glaciation, the most extensive and longest glaciation of the entire Phanerozoic (23). These results further support the idea that the atmospheric greenhouse effect has been a major factor affecting global climate change over geologic time.

#### REFERENCES AND NOTES

1. H. C. Urey, *The Planets: Their Origin and Development* (Yale Univ. Press, New Haven, CT, 1952).
2. C. I. Mora, S. G. Driese, P. G. Seager, *Geology* **19**, 1017 (1991); C. I. Mora and S. G. Driese, *Eos* **73**, 95 (1992); *Chem. Geol.*, in press.
3. C. J. Yapp and H. Poeths, *Nature* **355**, 342 (1992).
4. K. Caldeira and J. F. Kasting, *ibid.* **360**, 721 (1992).
5. R. A. Berner, *Am. J. Sci.* **291**, 339 (1991).
6. \_\_\_\_\_, *ibid.*, in press.
7. R. J. Oglesby and B. Saltzman, *Geophys. Res. Lett.* **17**, 1089 (1990).

8. R. J. Oglesby and S. Marshall, in *Modeling of Global Climate Change and Variability* (Max Planck Institute for Meteorology, Hamburg, 1992), p. 153.
9. M. E. Raymo, *Geology* **19**, 344 (1991).
10. F. M. Richter, D. B. Rowley, D. J. DePaolo, *Earth Planet. Sci. Lett.* **109**, 11 (1992).
11. P. V. Brady, *J. Geophys. Res.* **96**, 18101 (1991).
12. M. A. Velbel, in preparation.
13. T. Dunne, *Nature* **274**, 244 (1978).
14. N. E. Peters, *U.S. Geol. Surv. Water-Supply Pap.* **2228** (1984).
15. B. Otto-Bliesner, in preparation.
16. S. M. Stanley, *Earth and Life Through Time* (Freeman, New York, 1986).
17. R. A. Berner, *Geochim. Cosmochim. Acta* **56**, 3225 (1992).
18. D. W. Schwartzman and T. Volk, *Nature* **340**, 457 (1989).
19. J. I. Drever and J. Zobrist, *Geochim. Cosmochim. Acta* **56**, 3209 (1992).

20. From field studies M. F. Cochran and I have also found greatly enhanced initial weathering of basalt on the island of Hawaii due to the presence of higher plants.
21. R. A. Berner and D. E. Canfield, *Am. J. Sci.* **289**, 333 (1989).
22. The enhanced burial of organic carbon resulted in extra O<sub>2</sub> production. However, this production was largely compensated by diminished sedimentary pyrite burial, enhanced pyrite weathering, or both, at this time; see R. M. Garrels and A. Lerman, *Am. J. Sci.* **284**, 989 (1984).
23. T. J. Crowley and G. R. North, *Paleoclimatology* (Oxford Univ. Press, Oxford, 1991).
24. I thank C. I. Mora, S. G. Driese, R. J. Oglesby, M. A. Velbel, B. Otto-Bliesner, E. K. Berner, and M. F. Cochran for discussions and for providing data. Supported by National Science Foundation grant EAR 91-17099.

5 February 1993; accepted 20 April 1993

## Detection of Interstellar Pick-Up Hydrogen in the Solar System

G. Gloeckler, J. Geiss, H. Balsiger, L. A. Fisk, A. B. Galvin, F. M. Ipavich, K. W. Ogilvie, R. von Steiger, B. Wilken

Interstellar hydrogen ionized primarily by the solar wind has been detected by the SWICS instrument on the Ulysses spacecraft at a distance of 4.8 astronomical units from the sun. This "pick-up" hydrogen is identified by its distinct velocity distribution function, which drops abruptly at twice the local solar wind speed. From the measured fluxes of pick-up protons and singly charged helium, the number densities of neutral hydrogen and helium in the distant regions of the solar system are estimated to be  $0.077 \pm 0.015$  and  $0.013 \pm 0.003$  per cubic centimeter, respectively.

As the solar system moves through the local galactic cloud, some interstellar atoms can penetrate as far in as the orbit of Earth. These neutrals, approaching the sun, follow orbits determined by the combined force of gravitational attraction and solar radiation pressure before being ionized by the solar wind and energetic solar photons. The radial distance from the sun at which a substantial fraction of neutrals has been singly ionized is different for various interstellar atoms, depending on ionization cross sections that in turn scale roughly as the first ionization potential of the atom. Helium atoms, whose ionization potential is high, penetrate as far in as ~0.5 astronomical unit, whereas hydrogen gas, and to a lesser degree neutral oxygen, nitrogen, and neon, are excluded from regions closer than several astronom-

ical units (AU) from the sun. Singly charged pick-up helium of interstellar origin was discovered in 1984 at the orbit of Earth by means of a time-of-flight (TOF) instrument on board an Earth-orbiting spacecraft (1).

From measurements of light scattered from neutral interstellar hydrogen and known ionization processes in the heliosphere, pick-up hydrogen has long been inferred to exist at distances beyond several AU from the sun (2-4). However, direct evidence for its existence has been elusive, in spite of its dynamical importance in the solar wind. The detection of interstellar pick-up hydrogen poses an experimental challenge, requiring access to distances beyond several AU as well as appropriate instrumentation, such as a TOF ion composition spectrometer (5) with low background. Even then the separation of pick-up H<sup>+</sup> from the far more abundant solar wind protons is only possible when fluxes of suprathermal solar wind are sufficiently low, and because the two species have markedly different velocity distribution functions.

We report here the discovery of interstellar pick-up hydrogen. Our measurements were made using the Solar Wind Ion Composition Spectrometer (SWICS) (6)

G. Gloeckler, A. B. Galvin, F. M. Ipavich, Department of Physics, University of Maryland, College Park, MD 20742.

J. Geiss, H. Balsiger, R. von Steiger, Physikalisches Institut, Universität Bern, 3012 Bern, Switzerland.

L. A. Fisk, National Aeronautics and Space Administration, Office of Space Science and Applications, Washington, DC 20546.

K. W. Ogilvie, National Aeronautics and Space Administration, Goddard Space Flight Center, Greenbelt, MD 20770.

B. Wilken, Max-Planck-Institut für Aeronomie, 3411 Katlenburg-Lindau, Germany.

on board the Ulysses space probe (7), launched on 9 October 1990. SWICS is an energy-per-charge ( $E$ ) analyzer followed by a TOF ion mass spectrometer that uses an acceleration voltage ( $V_a = -23$  kV) to identify ions in space plasmas and measure their energy spectra from 0.6 to 60 keV per unit charge, corresponding to speeds from 340 to 3400 km s<sup>-1</sup> for H<sup>+</sup>, 170 to 1700 km s<sup>-1</sup> for He<sup>+</sup>, and similar velocity intervals for other heavy ions. During each spin period (12 s),  $E$  is sequentially selected from 64 logarithmically spaced steps, completing a cycle in  $\sim 13$  min. Although the prime objective of SWICS is to measure the composition of the solar wind, the coincidence techniques used reduce the background enough to allow the detection of pick-up ions. Because the flux of such ions was low they were identified using pulse-height data consisting of energy and TOF, as well as information on their arrival direction. From the TOF,  $E$ , and  $V_a$  the mass per unit charge (MPQ) of the ion is determined with a precision of about 8% ( $\Delta\text{MPQ}/\text{MPQ} \approx 0.08$ , full width-half maximum).

The measurements we report here were taken during a 15-day period (24 November to 9 December 1991) at a mean distance of 4.82 AU. Throughout this period the solar wind kinetic temperature was low and the flux of suprathermal solar wind protons (8) was far below the flux of pick-up H<sup>+</sup> (9). The average solar wind proton speed,  $V_{sw}$ , measured with SWICS was  $458 \pm 82$  km s<sup>-1</sup>, and its flux was  $3.8 \pm 1.3 \times 10^6$  cm<sup>-2</sup> s<sup>-1</sup>. Uncertainties are due to real variations in these quantities.

In our observations the average angle  $\gamma$  between the solar wind flow direction and the spacecraft spin axis was non-zero ( $\gamma = 12.6^\circ$ ), resulting in anisotropic angular distributions of protons and He<sup>+</sup> ions (Fig. 1). The curves labeled "Sphere" are fits to the data with  $\gamma = 12.6^\circ$ , assuming that the phase space densities in the reference frame moving with the solar wind (sw) frame are isotropic and homogeneous in a sphere of radius  $V_{sw}$  and zero elsewhere. This gives a good fit to the helium data but not to the proton data. A better fit to the H<sup>+</sup> angular distribution (labeled "Shell") is obtained by assuming that for pick-up protons the solar wind frame phase space density is isotropic, homogeneous, and non-zero only in a shell from  $\sim 0.8V_{sw}$  to  $V_{sw}$ .

The 15-day-averaged distribution functions,  $F(W)$ , measured in the spacecraft frame and plotted against the normalized ion speed,  $W = V_{ion}/V_{sw}$ , show sharp drops above twice the solar wind speed (Fig. 2). The general shapes of the observed distribution functions are in qualitative agreement with models predicting shell-like distributions for H<sup>+</sup> and sphere-like shapes for He<sup>+</sup>, in the solar wind frame (3).

In the reference frame of the local solar wind, newly created ions, moving initially with speed  $\sim V_{sw}$ , are subjected to the Lorentz force and will gyrate about the local interplanetary magnetic field (3). These pick-up ions are then convected outward by the expanding solar wind. In the spacecraft frame of reference the velocity of these pick-up ions will range between about 0 and  $2V_{sw}$ . The measured distribution functions (Fig. 2) have exactly this feature: a sharp cut-off at  $2V_{sw}$ . The correlation of the cut-off speeds of both H<sup>+</sup> and He<sup>+</sup> with the local solar wind speed is illustrated in Fig. 3.

The initial velocity distribution function

of pick-up ions is expected to be modified by pitch-angle scattering and energy diffusion at rates that depend on the characteristic times for these processes,  $\tau_\alpha$  and  $\tau_E$ , compared with the characteristic flow time,  $\tau_F = \Delta r/V_{sw}$ , of the pick-up ions (3). At  $\sim 5$  AU,  $\Delta r \sim 2$  AU for H<sup>+</sup> and  $\sim 4$  AU for He<sup>+</sup>. Thermalization of pick-up H<sup>+</sup> and He<sup>+</sup> ( $\tau_E < \tau_F$ ) is ruled out by our observations (Fig. 2) that pick-up H<sup>+</sup> and He<sup>+</sup> have speeds up to  $2V_{sw}$  [see also (1, 10) regarding previous observations of He<sup>+</sup>]. Weak pitch angle diffusion ( $\tau_\alpha > \tau_F$ ) is also ruled out as it would manifest itself by instances of cut-off speeds substantially be-

**Fig. 1.** Counts per sector plotted against spin phase angle for pick-up H<sup>+</sup> (upper panel) and He<sup>+</sup> (lower panel), measured in the spacecraft frame, from 24 November to 9 December 1991. Only protons with speeds above  $1.5V_{sw}$  and He<sup>+</sup> with speed above  $1.2V_{sw}$  ( $V_{sw}$  is the locally measured solar wind speed) have been included in these plots. In one spacecraft spin period (12 s) the  $4^\circ$  by  $60^\circ$  fan shaped field of view of SWICS, with one of its edges aligned on the Ulysses spin axis, sweeps out a  $120^\circ$  cone whose symmetry axis is directed toward Earth. This view cone is segmented into eight  $45^\circ$  azimuthal sectors and the sector number is recorded along with the pulse height data, thus providing some information on the arrival direction of ions. The SWICS instrument looks at the sun when the spin phase angle is  $0^\circ$ . During our observing period the angle between the average solar wind flow direction and the Ulysses-Earth vector was  $12.6^\circ$ , resulting in the observed anisotropy whose maximum lies in the solar direction. The He<sup>+</sup> anisotropy data in the lower panel are well fit by an isotropic "sphere" distribution of pick-up He<sup>+</sup> in the solar wind frame. The H<sup>+</sup> distribution in the upper panel is better fit by an isotropic "shell" distribution for pick-up hydrogen in the solar wind frame.

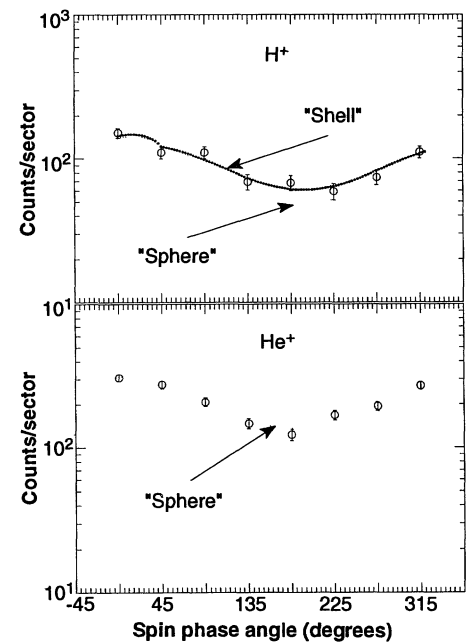
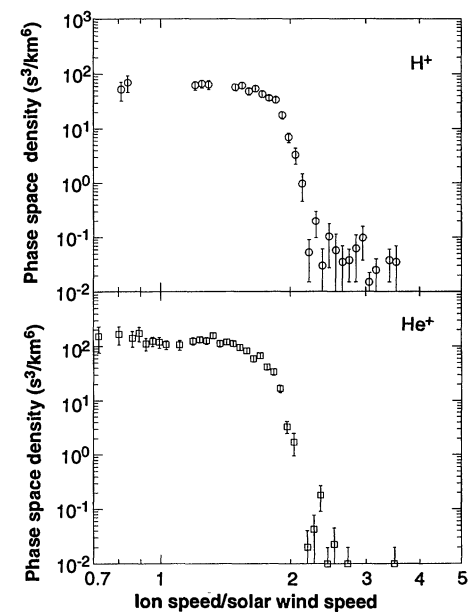


**Fig. 2.** Phase space density plotted against normalized ion speed,  $W = V_{ion}/V_{sw}$ , of interstellar pick-up hydrogen (upper panel) and pick-up helium (lower panel), measured in the Ulysses spacecraft frame with SWICS at a heliocentric distance of 4.82 AU, during the time period 24 November to 9 December 1991. These distribution functions,  $F(W)$ , were constructed by averaging individual 13-min, sector-averaged differential energy fluxes,  $(E \, dJ/dE)_i$ :  $F_i(W) = 0.545 \text{ (MPQ}_i/E)^2 E \, (dJ/dE)_i = \text{CF} \times C_i(E) \text{ (MPQ}_i/E)^2$ , where MPQ<sub>*i*</sub> is the mass per unit charge ratio of the ion,  $E$  is its energy per unit charge ratio, CF is the instrument response factor,  $C_i(E)$  is the count rate corrected for efficiency at a given  $E$  and  $W^2 = (438/V_{sw})^2 (E/\text{MPQ}_i)$ . Because energy/charge steps and sectors corresponding to solar wind velocities have been excluded from these data, the phase space density of H<sup>+</sup> around  $W \approx 1$  and  $W \approx 1.4$  is not available. Both spectra are characterized by a sharp decrease in phase space density at the cutoff speed  $V_c = 2V_{sw}$  to background levels. Below  $V_c$  the spectral shapes are somewhat different for pick-up H<sup>+</sup> and He<sup>+</sup> reflecting differences in the distribution functions of these ions in the solar wind frame.



low  $2V_{sw}$ , contrary to our data shown in Fig. 3. Furthermore, the rapid drop of  $F(W)$  beyond  $2V_{sw}$  (Fig. 2) indicates that energy diffusion (11) is small compared to adiabatic cooling. We conclude that for pick-up  $H^+$  as well as  $He^+$  (1), rapid pitch angle

scattering produces isotropic phase space densities in the solar wind frame, and that energy changes due to interaction with plasma waves are small ( $\tau_\alpha \ll \tau_F \ll \tau_E$ ). Strong pitch angle scattering leads to adiabatic cooling in the expanding solar wind,

in agreement with our observations (Fig. 2) of significant fluxes of pick-up ions below  $2V_{sw}$ .

At the location  $(r, \theta)$  of Ulysses, where  $r$  is the distance from the sun and  $\theta$  the angle between the sun-Ulysses vector and the direction of motion of the sun relative to the interstellar gas, the outward flux of pick-up ions of species  $i$  is

$$j_i^+(r, \theta) = N_i \beta_{i\text{prod}}(r_0/r)^2 \int_0^r (n_i(r', \theta)/N_i) dr'$$

where  $N_i$  is the interstellar neutral density,  $\beta_{i\text{prod}}$  is the ion production rate at  $r_0 = 1.5 \times 10^{13}$  cm (= 1 astronomical unit) and  $n_i(r', \theta)$  is the local neutral density (3). During our observations  $r$  was 4.82 AU and  $\theta$  was  $99^\circ$ . The values for  $j_i^+(r, \theta) = V_{sw} n_i^+(r, \theta)$  and number density,  $n_i^+(r, \theta)$ , of pick-up  $H^+$  and  $He^+$ , obtained from corresponding count rates, are given in Table 1. Using standard analytical expressions for  $n_i(r', \theta)/N_i$  (12) and parameter values listed in Table 1, we determine the neutral density,  $N_i$ , of H and He in the outer regions of the solar system to be  $0.077 \pm 0.015$  cm $^{-3}$  and  $0.013 \pm 0.003$  cm $^{-3}$ , respectively. The errors assigned to these densities do not include uncertainties in model parameters. These densities agree with estimates from EUV spectrophotometer measurements (13) and with direct measurements of the neutral helium density by Ulysses (14). Our H/He density ratio of  $6 \pm 1$  is more accurately determined than the individual absolute densities because systematic instrument uncertainties are reduced.

Pick-up ions are the most likely seed particles for the anomalous cosmic rays (ACR), which have energies  $\leq 50$  MeV per nucleon and an unusual composition, highly enriched in He, N, O and Ne (15). The detection of pick-up protons strengthens the case for the presence of ACR hydrogen (16). Our direct measurement of the pick-up  $H^+$  and  $He^+$  fluxes, combined with observation of the abundance of the ACR protons and helium, will provide information on the efficiency of the ACR acceleration mechanism.

Ultra-low-frequency waves are expected to be generated by pick-up hydrogen. For a pick-up  $H^+$  density of  $6 \times 10^{-4}$  cm $^{-3}$  at 7.5 AU, a factor of  $\sim 10$  enhancement in the solar wind wave spectrum at cyclotron resonant frequencies ( $10^{-2}$  Hz) was predicted (17). However, searches to detect such waves have as yet produced no clear evidence for their continuous presence (18–20). Our measured number density ( $n_{H^+} \approx 5 \times 10^{-5}$  cm $^{-3}$  at 4.8 AU), which is an order of magnitude lower, may provide a partial explanation of these results.

Finally, we note that our interstellar H/He ratio is lower than the generally accepted ratio of  $\sim 10$  (21). This may be

**Fig. 3.** (A) Time dependence of the cut-off speeds of pick-up  $H^+$  (open circles), pick-up  $He^+$  (open squares) and the solar wind speed (solid circles) for the 14 day period starting 24 November 1991. Each value of the cut-off speed,  $V_c$ , has been computed from the corresponding 6.5-hour differential energy flux, and represents the speed at which the energy flux dropped to half of its peak value. The error bars are determined from counting statistics. (B) Scatter plot of the cut-off speeds of pick-up  $H^+$  (open circles) and pick-up  $He^+$  (open squares) plotted against the local solar wind speed, using the data in the upper panel. The full and dotted lines are linear fits ( $V_c = s V_{sw}$ ) to the  $H^+$  and  $He^+$  data respectively. Best fit slopes are  $s = 1.96 \pm 0.05$  for  $H^+$  and  $s = 1.89 \pm 0.05$  for  $He^+$ .

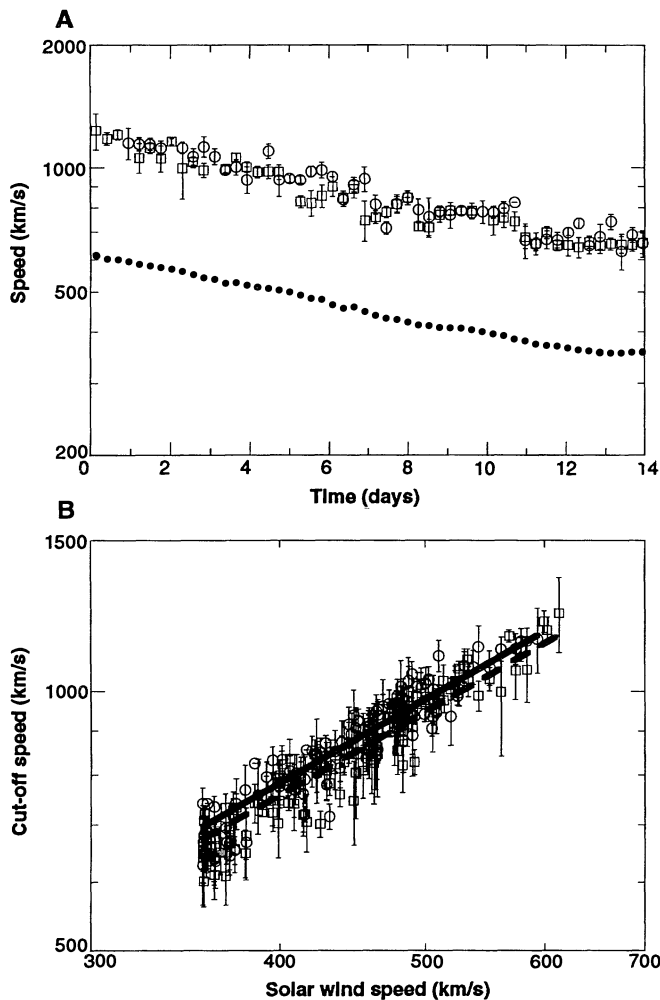


**Table 1.** Model parameters, measured characteristics of pick-up ions, and derived neutral densities.

Parameter	Symbol	$H^+$	$He^+$	Units
Local production rate at 1 AU*	$\beta_{\text{prod}}$	$3.5 \times 10^{-7}$	$1.0 \times 10^{-7}$	$s^{-1}$
Average loss rate at 1 AU†	$\beta_{\text{loss}}$	$8 \times 10^{-7}$	$1.0 \times 10^{-7}$	$s^{-1}$
Neutral gas speed	$V_c$	20‡	25§	km s $^{-1}$
Radiation/gravitation forces‡	$\mu$	1	0	
Pick-up ion flux at 4.82 AU	$j^+$	$2500 \pm 500$	$3100 \pm 600$	cm $^{-2}$ s $^{-1}$
Pick-up ion number density at 4.82 AU	$n^+$	$(5.4 \pm 1.1) \times 10^{-5}$	$(6.7 \pm 1.3) \times 10^{-5}$	cm $^{-3}$
Neutral density at 4.82 AU (from flux)	$n$	$0.0087 \pm 0.0018$	$0.011 \pm 0.002$	cm $^{-3}$
Neutral density in outer solar system	$N$	$0.077 \pm 0.015$	$0.013 \pm 0.003$	cm $^{-3}$

\*Value for H from (4) has been adjusted to reflect the lower than average solar wind flux measured during the observation period. †From (4). While it is generally assumed (as we do for  $He^+$ ) that  $\beta_{\text{prod}} = \beta_{\text{loss}}$ , this need not be the case, since flux averages over different time scales are involved. For  $\beta_{\text{loss}}$  a long-term (year or more) average is appropriate, while for  $\beta_{\text{prod}}$  a short-term (month or less) average should be used. ‡From (13). §From (14). ||Indicated errors include only systematic uncertainties in instrument response functions and statistical errors.

due in part to uncertainties in the assumed values of model parameters. It may also imply that charge exchange in the outer regions of the solar system removes some of the neutral hydrogen (22). More detailed analysis of pick-up ion data, planned for the future, should help to resolve these questions.

REFERENCES AND NOTES

1. E. Möbius *et al.*, *Nature* **318**, 426 (1985).
2. W. I. Axford, *Solar Wind* (NASA Spec. Publ., SP-308 Washington, DC, 1972), p. 609.
3. V. M. Vasyliunas and G. L. Siscoe, *J. Geophys. Res.* **81**, 1247 (1976).
4. T. E. Holzer, *Rev. Geophys. Space Phys.* **15**, 467 (1977), and references therein.
5. G. Gloeckler, *Rev. Sci. Instrum.* **61**, 3613 (1990).
6. G. Gloeckler *et al.*, *Astron. Astrophys. Suppl. Ser.* **92**, 267 (1992).
7. K.-P. Wenzel, R. G. Marsden, D. E. Page, E. J. Smith, *ibid.*, p. 207.
8. K. W. Ogilvie, J. Geiss, G. Gloeckler, B. Berdichevsky, B. Wilken, *J. Geophys. Res.* **98**, 3605 (1993).
9. Interstellar He<sup>+</sup>, on the other hand, is easily seen at all times because of the negligible amount of solar wind He<sup>+</sup>.
10. W. C. Feldman, J. R. Asbridge, S. J. Bame, P. D. Kearney, *J. Geophys. Res.* **79**, 1808 (1974).
11. P. A. Isenberg, *ibid.* **92**, 1067 (1987).

12. G. E. Thomas, *Ann. Rev. Earth Planet. Sci.* **6**, 173 (1978).
13. E. Chassefiere *et al.*, *Astron Astrophys.* **160**, 299 (1986).
14. M. Witte, H. Rosenbauer, M. Banaszekiewicz, H. Fahr, in *COSPAR Symp. on the Outer Heliosphere*, D. E. Page, Ed. (Pergamon, New York, in press).
15. L. A. Fisk, *Astrophys. J.* **206**, 333 (1976).
16. E. R. Christian, A. C. Cummings, E. C. Stone, *Astrophys. J. Lett.* **334**, L77 (1988).
17. M. A. Lee and W.-H. Ip, *J. Geophys. Res.* **92**, 11041 (1987).
18. E. J. Smith, *Adv. Space Res.* **9**, 159 (1989).
19. M. L. Goldstein and R. Lepping, *Eos* **73**, 246 (1992).
20. E. J. Smith *et al.*, *J. Geophys. Res.*, in press.
21. E. Anders and N. Grevesse, *Geochim. Cosmochim. Acta* **53**, 1197 (1988).
22. R. Osterbart and H. J. Fahr, *Astron. Astrophys.* **264**, 260 (1992).
23. We are grateful to the many individuals at the University of Maryland, the University of Bern, the Technical University of Braunschweig, the Max-Planck-Institut für Aeronomie, and the Goddard Space Flight Center who have contributed to the SWICS experiment. We have benefited from discussions with C. Gloeckler, J. R. Jokipii, M. A. Lee, E. Möbius, and E. C. Stone. This work was supported by NASA/JPL contract 955460, the Swiss National Science Foundation, and the Bundesminister für Forschung und Technologie of Germany.

19 January 1993; accepted 3 May 1993

# Directionally Aligned Helical Peptides on Surfaces

James K. Whitesell\* and Hye Kyung Chang

Directionally oriented peptide layers 1000 angstroms thick were constructed by polymerization on gold and indium-tin-oxide glass. A key feature is the use of an appropriately functionalized surface on which the initiation sites for polymerization are spaced at distances consistent with the helical diameter of the peptide. Completely helical polyalanine and polyphenylalanine layers have been constructed. The helicity of the polyalanine layer was completely retained after heating at 180°C for 7 days.

The rational design and preparation of materials for a wide range of practical applications, such as information storage and processing, requires protocols for the assembly of molecular units into supramolecular arrays. For example, optical switches based on second-order nonlinear effects require materials with unidirectional alignment of axes of molecular polarizability over domains that exceed the wavelength of the light (1-4). Several techniques for the alignment of organic materials have been investigated, making use of single-crystal materials, liquid crystals, Langmuir-Blodgett films, poled polymers, and host-guest inclusion complexes. However, none of the techniques have provided a satisfactory solution addressing all of the requirements for devices, including such practical issues as long-term stability to both heat

and light. Recent reports have described thin multilayers built by sequential deposition of monolayers (5), as well as thin films formed by the cross-linking of monolayers (6). We describe a complementary approach that provides a directionally organized assembly of large molecules built by polymerization on a gold surface.

Peptides have received little attention as optical switching materials, in part because methods that result in unidirectional alignment have been lacking (7-11). Nonetheless, a helical peptide has characteristics similar to crystalline urea, with a network of hydrogen bonds extending from one end of the chain to the other (Fig. 1) (12). Thus, we sought a method for the assembly of helical peptides for which the axes of all molecules point in the same direction. However, the helical arrangement is favored over the  $\beta$ -pleated sheet only when there are more than 10 amino acid residues in the polymer, and at that size, homogeneous peptides are quite insoluble. As a result, we

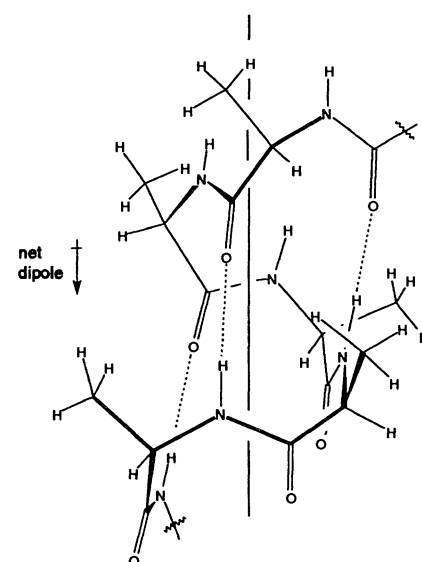
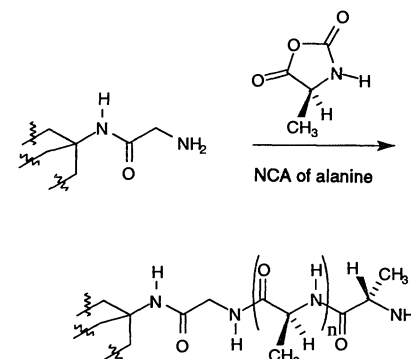


Fig. 1. Helical polyalanine showing the net macroscopic dipole resulting from the summation of the electrostatics of the individual, constituent amide groups.

focused our attention on the formation of peptides on a surface by in situ polymerization and chose the [100] face of gold as a relatively flat substrate to which suitable "seeds" could be attached and from which the polymers could be grown (13-15).

The interatomic spacing on the Au [100] surface is substantially smaller (4.1 Å) than the diameter of a helical peptide (~9 Å for polyalanine) (Fig. 2A). Thus, it is essential that the seeds deposited on the surface each occupy at least 9 Å; to this end, we prepared the aminotrithiol (16) "tripod" 1 (Fig. 2B). This compound adheres tightly to evaporated gold surfaces (on a thin layer of chromium on silicon), and treatment of such a surface-bound layer of 1 with the N-carboxyanhydride (NCA) of alanine in acetonitrile led to the growth of a substantial layer of polyalanine.



The thickness and helicity of this material can be determined by comparison of the grazing-angle Fourier transform infrared (FTIR) spectrum (17) of this layer (Fig. 3A) with, respectively, a commercial sample of polyalanine (Fig. 3B) and a layer of

Department of Chemistry, University of Texas, Austin, TX 78712.

\*To whom all correspondence should be addressed.